Trends in Performance Improvements of a Coaxial Gas-Fed Pulsed Plasma Thruster*

J.K. Ziemer† and E.Y. Choueiri‡
Electric Propulsion and Plasma Dynamics Laboratory (EPPDyL)
Princeton University

Daniel Birx
Science Research Laboratory Inc.

IEPC-97-040§

Abstract

The performance of a coaxial gas-fed pulsed plasma thruster is shown to improve with increasing capacitance. We report experimental results which show that raising the capacitance from 94 μF to 180 μF at a pulse energy of 5 J has uniformly increased the thrust efficiency over all specific impulses by a factor of 1.2. Thrust efficiencies as high as 69% were attained. This increase, however, is below the predicted trend from a simple analytical impulse model. To understand this discrepancy and explore other trends, a more detailed one-dimensional numerical model was developed. This model uses an RLC circuit potential equation for the discharge electrical characteristics and a snow-plow model for mass accumulation. From this analysis it is clear that the dynamic efficiency of the gas sweeping process plays an important role in determining the effect of increasing capacitance on performance. By comparing the trends predicted by the one-dimensional numerical model with the measured data it was possible to infer that the limited performance improvement may be blamed on the increased capacitance causing the discharge to reach the edge of the electrodes before the capacitor is fully discharged.

*Research supported by Science Research Laboratory Inc. through a NASA-JPL SBIR. Portion of the work was also supported by the Air Force Office of Scientific Research, grant number: F49620-95-1-0291.

†Graduate Student, Research Assistant. Member AIAA.

‡Chief Scientist at EPPDyL. Assistant Professor, Applied Physics Group. Senior Member AIAA.

§Presented at the 25^{th} International Electric Propulsion Conference, Cleveland, OH, August 24-28, 1997.

1 Introduction

Gas-fed pulsed plasma thrusters (GFPPTs) have resurfaced as a highly efficient, low power method for propulsion[1]. Heavily studied in the early and middle 1960's, GFPPTs have long been associated with high performance[2, 3]. At one point efficiencies surpassed 50% at an I_{sp} near 5000 s using close to 65 J of stored energy per pulse[4]. However, at that time propellant utilization was an insurmountable problem with pulse durations that were much shorter than the time response of available space-qualified fast acting gas valves. Recently, work at Science Research Labs (SRL) and Princeton University's Electric Propulsion and Plasma Dynamics Lab (EPPDyL) has included designing and testing a new series of GFPPTs and power conditioning equipment which pulses the thruster at a sufficient rate to alleviate this difficulty. In addition, with the demand for low power and reduced mass devices, target operating conditions have been pushed to below ten joules per pulse while, at the same time, trying to achieve the beneficial combination of high efficiency with a reasonable specific impulse. Although high thrust to power (impulse to energy) ratios have been demonstrated over thirty years ago, these performance levels were achieved at much higher energies than the current studies. The focus of this research is to eventually produce a highly efficient device (>50%) with useful values of specific impulse (<5000 s) at low energies (near and below 1 J).

At the present time, four iterations of SRL-GFPPTs have been tested with the fifth in the fabrication phase. Development has been mainly em-

pirical with multiple design modifications leading to the most recently tested SRL4-GFPPT. The SRL4-GFPPT has the ability to operate with different amounts of capacitance. Two values have been studied so far: 93.7 μF and nearly twice that value, 180 μF. Results from the 93.7 μF configuration were presented recently in ref. [1]. Since then, the 180 μF configuration was tested and the results will be shown in this paper along with the previous data. Trends from this experimental data show that while the efficiency at a given specific impulse increased with increasing capacitance, it did not increase as much as predicted by a simple parametric analysis.

A more detailed numerical model has been developed to try to explain the performance trends of these devices. This model has, for the time being, been kept as simple as possible in order for it to be useful as a flexible tool for explaining the trends, scaling and performance relations brought out by the data. At this stage, the theoretical work described in this paper does not claim to be an exact representation of a particular GFPPT design; rather it is an attempt at answering specific questions about the trends found in the experimental database.

After a brief description of the the SRL4-GFPPT (more details are given in ref. [1]), we present and discuss the latest set of experimental data along with the previous data at half the capacitance. We then study the trends using, first, a simple model derived analytically from simplified expressions and averaged quantities. A more detailed one-dimensional model based on the basic dynamic principles is then presented followed by a discussion of the trends found from its numerical solution for conditions similar to those of the experiments. We conclude with a discussion of the model's limitations and future improvements

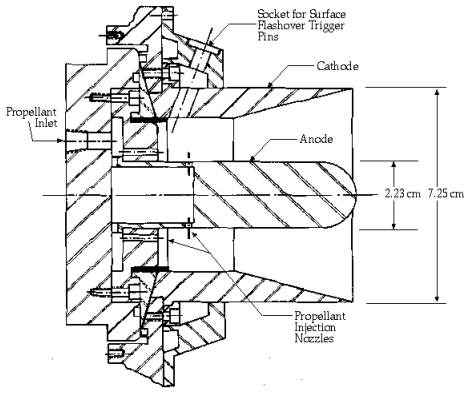

Figure 1: Schematic of the SRL4-GFPPT.

2 Performance Measurements

The SRL4-GFPPT. Since we have recently[1] described many of the characteristics of the SRL4-GFPPT we will only repeat the most pertinent details here. A schematic of the thruster is shown in figure 1. This geometry allows for an increase of inductance near 12 nH with the thruster electronics having an initial inductance of close to 5 nH. The thruster is controlled by an all-steady-state modulator and a separate high voltage triggering system. Energy for each discharge pulse is stored in a modular group of metal foil capacitors near the electrodes to minimize initial inductance. The all-solid-state control modulator can be set to produce pulse trains at rates up to 5000 pulses per second (pps) between 1-10 J per pulse. The modular discharge capacitors in the thruster housing can be switched in and out to create a total capacitance in multiples of approximately 45 μF up to 270 μF. To date, two configurations with two and four capacitor modules have been tested. In these experiments the initial stored energy is close to five joules with operating voltages of 330 V and 240 V for the 94 μF and 180 μF cases, respectively. Peak currents are near 12 kA in both cases with typical discharge times on the order of 3-5 μs. Sample voltage and current traces can be found in ref. [1]. The SRL4-GFPPT uses a pulsing scheme (also described in ref. [1]) that does not require high speed propellant injection control for a high degree of propellant utilization. This scheme relieves the requirements of fast response time for the gas valve and allows for a mass utilization efficiency close to 100%.

Experimental Conditions. The performance of the SRL4-GFPPT was measured with two values of capacitance (93.7 μF and 180 μF) keeping the mass bits and stored energy nearly the same between the configurations. For a performance calculation, three measurements are required for each individual pulse: the stored energy, mass bit, and impulse bit. For all data presented in this paper, a train of six pulses was fired per trial at close to 274 μs intervals. All results consist of what would be the average value of a single pulse in that train. The techniques for finding these average per-pulse values have been described previously in ref[1] and will only be summarized here.

Impulse Measurement. The impulse produced by the SRL4-GFPPT is measured by monitoring the position of the thruster mounted at the end of a swinging gate type thrust stand equipped with an RF proximeter and an interferometric proximeter system (IPS) for resolving. The impulsive thrust stand and impulse measurement techniques are described in refs. [5, 1]. For each data point at a different mass bit, ten trials of "cold" gas flow were taken without charging the capacitors yielding a cold gas impulse bit. These ten trials were averaged and compared to the expected cold gas velocity. Each individual impulse measurement has an error not greater than 3%. The standard deviation from trial to trial of cold gas impulses is also close to that value. For these data points, one trial was used for the "hot" impulse bit calculation. Again, from previous experiments with many hot pulses, the impulse bit magnitude has shown a shot to shot variation of about 8% near the impulse bit values presented in this paper. This is the value that will be used for the error on each impulse bit measurement.

Energy and Mass Bit Calculation. The average energy for each of the pulses was found by taking the charging voltage trace and using peak values of voltage before each discharge with $E = \frac{1}{2}CV_0^2$. The mass bit was calculated from choked flow considerations of a sonic orifice located near the thruster. The orifice was calibrated and the mass flow rate as a function of plenum pressure was found to be very linear. The mass bit is taken to be the mass flow rate times the period between pulses. This is, at worst, an overestimation of the actual mass bit as some of the gas will have time to leave the thrust chamber after 274 μs with a typical Argon cold gas velocity of 400 m/s.

Error Analysis. The largest source of error is the assumed standard deviation in the impulse measurement, 8%. The mass bit is accurate within 2% and the standard deviation of the individual pulse energy within a pulse train is 4%. Consequently the efficiency will have an error within 9.2% of its value and the specific impulse will be within 8.3% of its value.

Experimental Results. The results from both capacitance configurations are shown in figure 2 with tabulated results for the 180 μF configuration shown in table 2. Tabulated data for the 93.7 μF configuration was presented in the last paper[1]. Comparison of the two configurations yields some interesting trends.

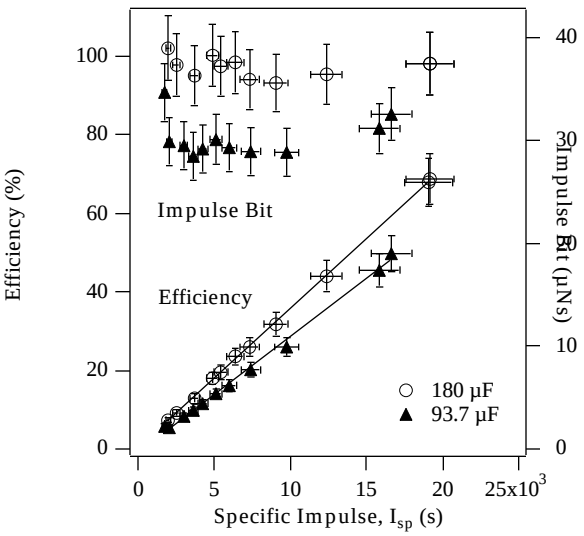

Figure 2: Measured performance data for the SRL4-GFPPT at a discharge energy of 5 Joules.

First, from figure 2 efficiency is shown to be generally higher with the higher value of capacitance. In fact, the highest efficiency point is nearly 70% with an I_{sp} of 19,100 s using 0.2 μg of propellant per pulse. At the 50% efficiency level, the specific impulse has been reduced from 17,000 s to about 14,000 s by doubling the capacitance. At a reasonable specific impulse, say 5000 s, the efficiency has increased from 14.7% to 17.8% by doubling the capacitance. By the linear relation seen in the results, $\eta \propto I_{sp}$, the efficiency to specific impulse ratio (equivalent to half the impulse bit to energy or thrust to power ratio, see equation 7) has increased by a factor of 1.21 or about 20% by doubling the capacitance.

Second, from figure 2 the impulse bit is shown to increase for the higher value of capacitance at close to the same stored energy. On average, the impulse bit increased by a factor of 1.25 by doubling the capacitance and using a slightly lower energy. Also, the impulse bit is found to be generally constant for a given capacitance and geometry as typical of an electromagnetic accelerator. Some fine structure depending on specific impulse is notably similar in both configurations although this is within the error of the measurements. In any case, the impulse to energy (thrust to power) ratio has increased from 5.6 μN/W to 7.3 μN/W on average by doubling the capacitance. This represents an increase in T/P by a factor of 1.3.

It is also relevant to note that based on a 0.8 μg/C

m_{bit} (μg)	I_{bit} (μN-s)	I_{sp} (s)	η (%)
0.2	37.5	19100	68.8
0.2	37.5	19100	67.7
0.3	36.4	12400	44.0
0.4	35.6	9080	31.7
0.5	36.0	7350	25.9
0.6	37.5	6380	23.4
0.7	37.2	5420	19.7
0.8	38.3	4880	18.0
1.0	36.3	3700	12.9
1.5	37.3	2540	9.1
2.0	38.9	1990	7.3
$\pm$2%	$\pm$8%	$\pm$8.3%	$\pm$9.2%

Table 1: SRL4-GFPPT Performance Data for a fixed energy of 5.1$\pm$0.2 J with a capacitance of 180 μF. The last row in the table is the error from each measurement.

erosion rate measured at JPL on a similar type of thruster at similar operating conditions, the fractional contribution of eroded mass to the total mass bit used by the thruster ranges between 1 and 10%. This effect is, at worst, in the outer limits of the error bars on the measured data.

3 Analytical GFPPT Performance Model

In a first attempt to study the trends in the measured data, we begin by developing a very simple analytical model. We start with a familiar expression for the impulse created by a Lorentz force,

$$I_{bit} = \frac{\mu_0}{4\pi} \ln\left(\frac{r_{out}}{r_{in}}\right) \int_0^t J^2 dt. \tag{1}$$

Estimating the integral by the expression, $< J^2 > \Delta t$, and further assuming that the current is simply the average rate of charge leaving the capacitor over the time length of the discharge, $J \approx CV_0/\Delta t$ then,

$$I_{bit} = \frac{\mu_0}{4\pi} \ln\left(\frac{r_{out}}{r_{in}}\right) \frac{C^2 V_0^2}{\Delta t}. \tag{2}$$

Next we replace $\frac{1}{2}CV_O^2$ by the energy and estimate the time length of the discharge to be an LC circuit time constant, $\Delta t \approx \sqrt{< L > C}$. This relation assumes that the resistance in the circuit is small and that the inductance, L, can be replaced by an average quantity, $< L >$. Using these two relations yields,

$$I_{bit} = \frac{\mu_0}{2\pi} \ln\left(\frac{r_{out}}{r_{in}}\right) \frac{EC}{\sqrt{< L > C}}. \tag{3}$$

The final step is to replace average inductance quantity with an inductance per unit length term times a characteristic length of acceleration. This characteristic length has some relation to the minimum length of electrodes, $< l_{elec} >_{min}$. In any case, the inductance per unit length of a coaxial device is,

$$L_1 = 2 \times 10^{-7} \ln\left(\frac{r_{out}}{r_{in}}\right). \tag{4}$$

This gives our last expression for the impulse bit,

$$I_{bit} = \left[2 \times 10^{-7} \ln\left(\frac{r_{out}}{r_{in}}\right)\right]^{1/2} \frac{E\sqrt{C}}{\sqrt{< l_{elec} >_{min}}}. \tag{5}$$

This expression does not depend on the mass bit which would seem to agree with the experimental data of impulse bit vs. specific impulse (figure 2) which was created by varying the mass bit. Also, it can be easily re-arranged to give the impulse to energy (thrust to power) ratio,

$$\frac{I_{bit}}{E} = \frac{T}{P} = \left[2 \times 10^{-7} \ln\left(\frac{r_{out}}{r_{in}}\right) \frac{C}{< l_{elec} >_{min}}\right]^{1/2}. \tag{6}$$

This relation is *only* dependent on the capacitance and the geometry of the discharge. It predicts an increase in the thrust to power ratio by a factor of about 1.4 compared to the measured factor of 1.3.

Considering the efficiency, we can write

$$\frac{I_{bit}}{E} = \frac{m_{bit} u_e}{\frac{1}{\eta}\frac{1}{2} m_{bit} u_e^2} = \frac{2\eta}{u_e} \propto \sqrt{C}. \tag{7}$$

In combination with eqn. 6, this model predicts that the efficiency is linearly proportional to the exhaust velocity (or specific impulse). It also predicts the efficiency to be proportional to the square root of the capacitance at a fixed specific impulse. This gives a predicted improvement factor for the performance of 1.4, however, only a factor 1.2 was measured. Clearly, this predicted trend could not continue indefinitely with enormous values of capacitance; in fact, it already appears to be over-estimating expected improvements.

Although this model does point out specific trends that are noticeable in the data (i.e. constant I_{bit} with changing mass bit, $\eta \propto I_{sp}$, etc.) it over-predicts

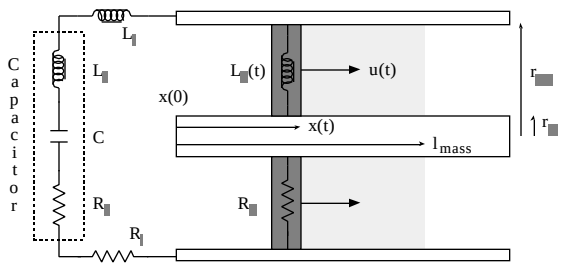

Figure 3: RLC circuit model and snow plow model representation. The electrodes can extend to an arbitrary length while the extent of the propellant is set by the parameter l_{mass}.

the performance improvements with increasing capacitance. In an attempt to understand these limitations we present a more comprehensive view of the discharge dynamics that results in a numerical model for solving these more complex relations.

4 Discharge Dynamics

Basic models for pulsed plasma thrusters that include a circuit model for the discharge potential and a "snow plow" model for the gas accumulation during the discharge exist in the literature[6, 7]. In this section we will go over the basic principles of these models and write the equations which will be solved later by numerical methods. A scheme for the discharge is shown in figure 3.

Discharge Potential. Treating the discharge as an RLC circuit with changing inductance produces a very simple and convenient model for the discharge potential. Adding the series inductance and resistance into two equivalent elements, $L(t) = L_c + L_l + L_p(t)$ and $R = R_c + R_l + R_p$, allows a compact form of Kirchhoff's Law to be expressed as,

$$V_0 = \frac{1}{C}\int_0^\tau J dt + \frac{d}{dt}(LJ) + RJ, \tag{8}$$

with variables including the current, J, and inductance, L, being a function of time while the capacitance, C, and resistance, R, are constant. In the case of co-axial electrodes with an azimuthally symmetric discharge, the inductance can be thought of as an initial inductance plus an inductance per unit length times the position of the current sheet, $L = L_0 + L_1 x$. The inductance per unit length, L_1 is shown in equation 4. Inserting this relation for the inductance into equation 8 and carrying out the differentiation leads to,

$$V_0 - \frac{1}{C}\int_0^\tau J dt = (L_1\dot{x} + R)J + (L_0 + L_1 x)\dot{J}. \tag{9}$$

This equation states that the voltage on the capacitor at any instant is divided between the changing inductance, the resistance, and the changing magnetic field.

Conservation of Momentum. A one dimensional equation for conservation of momentum with a Lorentz force is,

$$\frac{d}{dt}(mv) = F = \frac{1}{2}L_1 J^2. \tag{10}$$

Assuming that as the current sheet travels down the electrodes all the mass is swept up and contained in the sheet, the mass of the sheet will be increasing with time and the conservation equation can be written as,

$$m\ddot{x} = \frac{1}{2}L_1 J^2 - \dot{m}\dot{x}. \tag{11}$$

With a uniform gas density, the mass can be written as an initial mass and a mass per unit length times distance, (similarly to the inductance) $m = m_0 + m_1 x$, then the final equation can be written as,

$$(m_0 + m_1 x)\ddot{x} = \frac{1}{2}L_1 J^2 - m_1\dot{x}^2. \tag{12}$$

This equation shows that the acceleration of the mass in the current sheet is proportional to the Lorentz force minus a "drag" term that describes the loses associated with accumulating mass that was initially at rest. This has previously been described under the terms of a dynamic efficiency[8],

$$\eta_d = \frac{m_f \dot{x}_f^2}{\int_0^{t_f}(\dot{m}\dot{x}^2)dt + m_f\dot{x}_f^2} \tag{13}$$

Power and Energy Balance. Multiplying equation 9 for the voltage of the capacitor by J yields the distribution of power in the rest of the circuit,

$$P = (L_1\dot{x} + R)J^2 + (L_0 + L_1 x)\dot{J}J, \tag{14}$$

which after some rearranging yields,

$$P = \frac{1}{2}L_1\dot{x}J^2 + \frac{d}{dt}\left(\frac{1}{2}LJ^2\right) + RJ^2. \tag{15}$$

Multiplying equation 12 by the sheet velocity, $\dot{x}$, allows the first term in the power equation to be replaced:

$$P = \frac{d}{dt}\left(\frac{1}{2}m\dot{x}^2\right) + \frac{1}{2}\dot{m}\dot{x}^2 + \frac{d}{dt}\left(\frac{1}{2}LJ^2\right) + RJ^2. \quad (16)$$

This equation states that at any given instant, the power from the capacitor is used to change the kinetic energy of the discharge, heat up the discharge through mass accumulation, change the magnetic field, and heat up the plasma through resistive losses. Obviously, the beneficial term in this equation is changing kinetic energy. Integrating the power yields the partition of energy over the whole discharge time,

$$E = \left(\frac{1}{2}m\dot{x}^2\right)_f + \int_0^{t_f}\left[\frac{1}{2}\dot{m}\dot{x}^2 + RJ^2\right]dt, \quad (17)$$

where the current has been assumed to be zero at the beginning and end of the discharge so that any power going into changing the magnetic field is recovered. Here we see that the initial energy stored in the capacitor is broken up between plasma kinetic energy and two loss terms including a dynamic loss (see eq. 13) and a resistive loss. The energy that is partitioned for these two loses goes into heating up the plasma and is considered unrecoverable.

5 Numerical Solutions

In the work presented here we will not use the model as an accurate predictive tool for the performance of GF-PPTs since that would require a more rigorous specification of various free parameters such as various initial conditions, ending conditions, density profiles, and conductivity as well as the inclusion of two-dimensional effects. This is the subject of ongoing work. Instead, we focus on the study of typical *trends* as may be depicted by assuming uniform density, constant resistance, and infinitely long electrodes.

Equations 9 and 12 have been solved numerically through a simple time-stepping routine that has second order accuracy over 1000 time steps each being 20 ns long. This combination of points and time step size was found after many convergence trials. Increasing the number of points or shortening the time step do not significantly change the output of the numerical solution.

5.1 Initial Parameters and Model Validation

Solving these two coupled differential equations requires the input of some parameters including the source capacitance, the ambient gas density or mass bit, the geometry, the mass length (l_{mass}), the resistance, and the initial conditions. Throughout all results presented here, only the capacitance, initial voltage (all trials occur at five joules), and mass bit were varied. The other parameters were set as follows:

Geometry The geometry was set to have the same inner and outer electrode radii as the SRL4-GFPPT. The electrode length was not fixed allowing the plasma sheet to continue to conduct and move freely until the capacitor was fully discharged.

Mass Length The mass length was used to set the extent of the propellant within the electrodes. Especially for high capacitance discharges, the acceleration length was much longer than the extent of the propellant. In order to have reasonably similar gas densities, however, a length of 10 cm was chosen, $l_{mass} = 0.1$. The implications of this method are discussed in future sections (sect. 5.2).

Resistance The resistance was set at a constant 10 mΩ to match typical experimental peak current measurements. Varying the resistance slightly has a large affect on the predicted performance. For continuity, the resistance value was kept the same for all cases. In the future, a more realistic model of the plasma conductivity will replace the constant value.

Initial Conditions Initial conditions for this model are as follows: the current sheet is initially at rest, $x(0) = 0$, $\dot{x}(0) = 0$, $\ddot{x}(0) = 0$, and the current is zero, $J(0) = 0$ with a first derivative, $\dot{J}(0) = V_0/L_0$. The initial inductance was set at 5 nH in approximation of the initial inductance found in the SRL4-GFPPT. The initial mass was set as a 10% fraction of the total mass bit corresponding to 1 cm worth of gas volume.

5.2 Results

Figure 4 shows the efficiency and impulse bit as a function of specific impulse in a similar fashion to figure 2 for the experimental results. While the magnitudes are close to those of the measured data, the

experimentally found trends of a constant impulse bit and a linear relation between efficiency and specific impulse are not present. At the same time, an increase in efficiency and an increase in impulse bit is noticed for higher capacitor values, although the rate of increase is very small. The numerical model predicts an increase in efficiency at 5000 s I_{sp} of only 1% from 21% to 22% by doubling the capacitance. This represents a factor of 1.05, far *below* experimental results. Finally, one of the most important features to notice is the character of the efficiency curve. At the lower specific impulses, the slope of the curve matches well with experimental data. Above approximately 5000 s, however, the departure from the data increases.

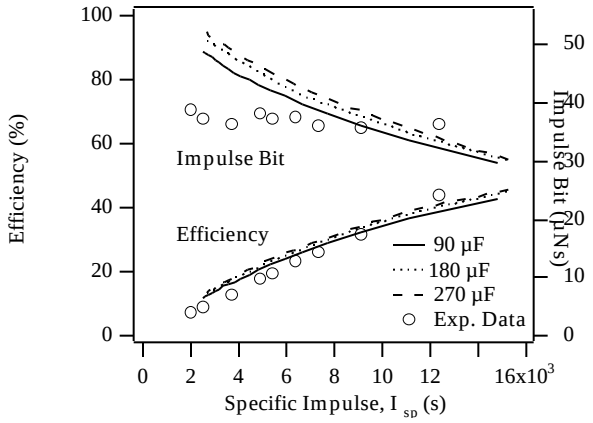

Figure 4: Simulated efficiency and impulse bit versus specific impulse with variable capacitance values at a discharge energy of 5 joules. Experimental data from the 180 μF SRL4-GFPPT is also shown.

The efficiency of the thruster operating at a specific impulse of 5000 s is examined more closely in figure 5. Here the efficiency is shown to increase with capacitance although much slower than predicted by eq. 7 and with a drastic slope change over the range of simulated capacitances. Two possible reasons for this decrease in performance were proposed and examined: a dynamic efficiency loss or a problem of electrode length.

Dynamic Efficiency The dynamic efficiency of the mass accumulation was recorded and plotted on figure 5 using equation 13. From that equation,it is clear that in order to achieve high efficiency the mass must be accumulated early (and as slowly as possible) when the velocity is small.

For a constant distribution of propellant, the mass flow rate is proportional to the velocity which makes the power going into this loss related to $\dot{m}\dot{x}^2 = m_1\dot{x}^3$ where m_1 is the mass per unit length. This makes the inefficiency proportional to the integral of the velocity cubed. It appears as though a slow gradual acceleration with most of the mass being accumulated early would be the best situation. For many of the larger capacitances, this is exactly the case. Large capacitance have a long enough time constant that the current sheet can move out of the propellant zone, past 10 cm of electrodes and propellant volume, into free space where no more mass will be accumulated. At this point, some kinetic energy can still be added to the discharge through the electrodes. The dynamic efficiency is high for these cases simply because after the current sheet passes l_{mass} it gains no more mass while continuing to be accelerated electromagnetically. Obviously, this is not the case in reality with thrusters that have finite electrode lengths. This points to the question of how much impulse does the current sheet actually receive before it reaches the end of the mass length, or in the case of the real SRL4-GFPPT, before it reaches the end of the electrodes?

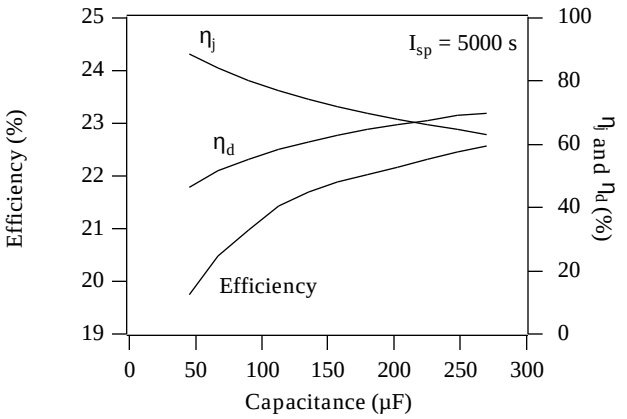

Figure 5: Efficiency as a function of capacitance at 5000 s I_{sp}. Dynamic (η_d eq. 13) and current (η_j eq. 18) efficiencies are also included.

Acceleration Length To answer that question, we define a new efficiency describing the amount of impulse (relative to the total impulse) given to the discharge before reaching the end of the propellant

length, $x = l_{mass}$,

$$\eta_j = \frac{\int_0^{\delta} J^2 dt}{\int_0^{t_f} J^2 dt}, \tag{18}$$

where δ is the time for the current sheet to reach l_{mass} ($x(\delta) = l_{mass}$) and t_f is the time for the capacitor to be fully discharged. The quantity $1 - \eta_j$ is the percentage of the final impulse bit provided to the discharge after it has accumulated all of its mass (after 10 cm in these simulations). The total acceleration length (equivalent to how long the electrodes would have to be) is $l_{accel} = x(t_f)$.

From the simulations many of the cases have longer acceleration lengths than mass lengths, $l_{accel} > l_{mass}$. This is especially true of the higher capacitance simulations where, as seen in figure 5, up to 40% of the impulse is yet to be supplied by the time the current sheet reaches the extent of the propellant. Even more important to note is the fact that the real thruster, the 180 μF SRL4-GFPPT, has 6.26 cm long electrodes and that the discharge could very well be reaching the end of the electrodes before the capacitor is fully discharged.

The model makes no claims of accuracy in predicting a discharge that, in reality, moves beyond the electrode edges. For that reason, the electrodes in the model were extended to infinity while the extent of the gas was limited to reasonable lengths. Therefore, any simulated data where $l_{accel} > l_{mass}$ (which typically corresponds to I_{sp} values greater than 5000 s) should not be considered as a true representation of experimental performance.

6 Conclusions

Performance of a coaxial gas-fed pulsed plasma thruster has been characterized at two values of the driving capacitance. Increasing the capacitance has been shown to increase thrust efficiency at a given specific impulse although not as much as expected from a simple analytical model that does not include dynamic efficiency losses. A more detailed numerical model was used to study trends and showed that dynamic efficiency plays an important role in determining the overall dependencies especially for large values of the capacitance where the discharge time length is long. In addition, the calculated trends pointed out that the discharge of the SRL4-GFPPT with 180 μF might be reaching the end of the electrodes before the capacitor is fully discharged possibly explaining part of below than expected performance.

In order to study the characteristics of GF-PPTs beyond general trends, a more accurate two-dimensional numerical model is being developed including the effects of nonuniform density profiles and a variable circuit resistance function.

References

[1] J.K. Ziemer, E.A. Cubbin, E.Y. Choueiri, and D. Birx. Performance characterization of a high efficiency gas-fed pulsed plasma thruster. In 33^{rd} *Joint Propulsion Conference*, Seattle, Washington, July 6-9 1997. AIAA 97-2925.

[2] B. Gorowitz, T.W. Karras, and P. Gloersen. Performance of an electrically triggered repetitively pulsed coaxial plasma engine. *AIAA Journal*, 4(6):1027–1031, June 1966.

[3] P. Gloersen. Current status of pulsed plasma engine development. In 2^{nd} *Joint Propulsion Conference*, Colorado Springs, Colorado, June 13-17 1966. AIAA 66-566.

[4] B. Gorowitz, P. Gloersen, and T.W. Karras. Steady state operation of a two-stage pulsed coaxial plasma engine. In 5^{th} *Electric Propulsion Conference*, San Diego, California, March 7-9 1966. AIAA 66-240.

[5] E.A. Cubbin, J. Ziemer, E.Y. Choueiri, and R.G. Jahn. Laser interferometric measurements of impulsive thrust. *Review of Scientific Instruments*, 68(6):2339–2346, 1997.

[6] P.J. Hart. Plasma acceleration with coaxial electrodes. *The Physics of Fluids*, 5(1):38–47, January 1962.

[7] C.J. Michels, J.E. Heighway, and A.E. Johansen. Analytical and experimental performance of capacitor powered coaxial plasma guns. *AIAA Journal*, 4(5):823–830, May 1966.

[8] N.A. Black and R.G. Jahn. Dynamic efficiency of pulsed plasma accelerators. *AIAA Journal*, 3(6):1209–1210, June 1965.